

# Geochemical evidence in support of sedimentary precursors to Proterozoic sillimanite-bearing rocks, Vest-Agder, South Norway

TORGEIR FALKUM & SIDSEL GRUNDTVIG

Falkum, T. & Grundvig, S. 2006: Geochemical evidence in support of sedimentary precursors to Proterozoic sillimanite-bearing rocks, Vest-Agder, South Norway. *Norges geologiske undersøkelse Bulletin 446*, 19–34.

Sillimanite-bearing alumina-rich schists and gneisses from three different areas within the Agder region in southern Norway are interpreted as having sedimentary precursors, transformed during deep-seated Sveconorwegian deformation and high-grade metamorphism which led to complete recrystallization, so that their precursors are now beyond recognition. The layers and lenses of rather rare occurrences of sillimanite-bearing schists and gneisses belong to the oldest recognisable layered formation of the Proterozoic rock sequence and are interlayered with quartzites and marbles in the easternmost localities. Major element analyses support the conclusion that the precursors were clay-dominated sediments derived from mafic rocks and to a varying degree mixed with more felsic rocks developed during extensive weathering in a relatively warm, humid climate. Trace element data also indicate the presence of an original clay fraction in the precursors and imply a high degree of continental source rocks. Distribution of the individual elements may be explained by physico-chemical parameters known to control element behaviour in sedimentary processes in connection with clay deposition.

Torgeir Falkum & Sidsel Grundvig, Geologisk Institut, Aarhus Universitet, DK-8000. Århus C, Denmark.

## Introduction

The Late Palaeoproterozoic to Mesoproterozoic of southern Norway is dominated by numerous plutons that were emplaced into a layered complex consisting mostly of gneisses and amphibolites. Most of the plutons suffered high-grade metamorphism and deformation during the Sveconorwegian orogeny, commonly during several phases of intense flow folding. Within the older banded gneiss complex, there are small and rare occurrences of irregular layers and lenses of sillimanite-bearing schists and garnet-sillimanite gneisses (Falkum 1966a, 1998) which have participated in all the recognisable phases of tectonic deformation. In other places granitic magma has assimilated most of the original rock leaving a granite with some relict metamorphic garnets. These peraluminous rocks all have low Ca and Na contents, thus facilitating the formation of sillimanite during high-grade metamorphism.

The main purpose of the present study has been to supplement the existing element geochemistry with new analyses in order to check if there is any pattern which may support a sedimentary origin of the precursors to these sillimanite-bearing rocks.

## Field occurrence and rock-types

Samples have been collected from three main areas approximately 75 km apart, in order to see if any regional variation may be established (Fig. 1). The easternmost area, at *Tveit*, is 10 km northeast of Kristiansand. In this area *biotite-garnet-sillimanite schist* occur interlayered with quartzites and nearby marbles within a banded gneiss sequence. The mar-

bles have been traced almost continuously and mapped for several tens of kilometres, suggesting a sedimentary origin with relative large lateral extent (Falkum 1966a). The association of extensive limestone together with large sand and clay deposits suggests a relatively stable near-continental environment. Seven samples were collected from a 20 m-high profile in banded gneisses in the western limb of the large *Tveit* antiform (samples G25-6 to 12). The biotite-garnet-sillimanite schist can be intermittently traced to the southwest and two samples were collected from *Gill*, which is 5 km southwest of *Tveit*. These samples (K23-17A & B) are considered to belong to the *Tveit* area.

The second main area is located on the Oftenes peninsula in the county of *Søgne*, roughly 15 km southwest of Kristiansand. A few metre thick layers of *biotite-garnet-sillimanite schist* can be followed for 40-50 m within a banded biotite gneiss-amphibolite sequence. Six samples were collected from this locality. Sample Oft-1 is from the border zone, whereas the others (Oft-2, 3, 4, and O19-50A & B) are from the central part of the layer along strike.

Sillimanite-rich schists and gneisses are the main metasedimentary lithologies in *Flekkefjord*. Another possible metasediment is an amphibolite with regular cm-thick quartz layers (Falkum 1966b, 1998). This lithology may represent either a graded metaturbidite deposit or basic ash layers alternating with sand layers. *Flekkefjord* is approximately 60 km farther west from *Søgne* and the distance between the easternmost and the westernmost sample localities is 75 km. Whereas the rocks in the former areas are metamorphosed in amphibolite facies, those in the *Flekkefjord* area

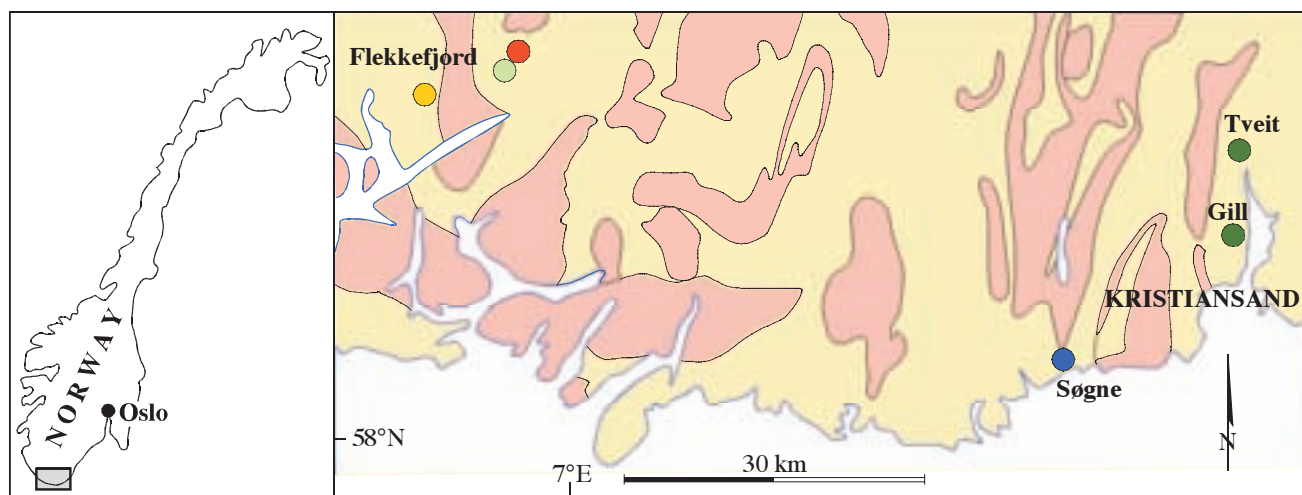


Fig. 1. Locations of the sampled sillimanite-bearing rocks in Agder, southern Norway. The oldest rock complex (yellow) contains different gneiss units, ranging from homogeneous to banded gneisses grading into biotite-dominated schists with sillimanite-rich layers. The younger intrusions (brown) are syn- to postkinematic granitic rocks. The inset map shows the location of the study area.

grade from amphibolite facies in the east to granulite facies in the west. All samples were collected inside the hypersthene isograd within the banded gneiss sequence.

Three different rock-types were collected from Flekkefjord. The first type, *biotite-garnet-sillimanite-cordierite schist* (samples A24-6; A24-31) is similar to the biotite-garnet-sillimanite schists from Tveit and Søgne. The second type belongs to a *quartz-rich gneissic* type with garnet, sillimanite and subordinate biotite and feldspars, referred to as quartz-sillimanite gneiss. Sample (Q30-3) has 65% SiO<sub>2</sub> and 40% normative quartz (CIPW norm). The other sample (Q29-12) has 75% SiO<sub>2</sub> and 55% normative quartz. The third type is also a leucocratic gneiss that is dominated by garnet and feldspar with subordinate sillimanite and biotite, referred to as *felsic garnet-sillimanite gneiss* or *felsic gneiss* (samples A24-27; A24-29). All these rock-types are found within the intensely deformed banded gneiss suite.

## Analytical methods

### X-ray fluorescence

Loss-on-ignition was determined by heating the powder in air in a muffle furnace at 950°C for 3 hours. Fused glasses were prepared by mixing 0.75 g of ignited sample with 3.75 g of Fluore-X65 HP (a commercial flux from Socachim Fine Chemicals consisting of 66 wt.% Li<sub>2</sub>B<sub>4</sub>O<sub>7</sub> and 34 wt.% LiBO<sub>2</sub>) in a 30 ml 95Pt-5Au crucible. The crucible was transferred to a muffle furnace and the contents melted twice for 5 minutes at 1150°C, with swirling of the crucible between melting. After fusion, the melt was poured into a red-hot, 32 mm 95Pt-5Au mould and quenched with air to produce a flat glass disc. The glass disc is used for the major analysis.

Powder pellets were prepared by mixing thoroughly 6 g of sample powder with 1.0 g phenol formaldehyde (British Bakelite Company; resin R0214). After mixing, the powder is placed in an X-ray die and pressed in a hydraulic press for 5 min at 30 tons. The pellet is placed in an oven operating at

110°C. After 30 min the phenol formaldehyde is set and the pellet is ready for trace element analysis.

The major and the trace element analyses were performed on a PANalytical PW2400 X-ray spectrometer using SuperQ software. For the major elements a 3 kW Rh-tube was used operating at 50 kV and 55 mA along with PX-1 multilayer for Na and Mg, PE crystal for Al and Si, Ge crystal for P, LiF(200) crystal for K, Ca and Ti and LiF(220) crystal for Mn and Fe. The detector was a gas-flow proportional counter using P10 (10% methane in Ar) gas. For Mn and Fe, this detector was used in tandem with a sealed Xe detector.

For the trace elements Ba, La, Ce, V and Cr the Rh tube was operated at 50 kV and 55 mA, for the rest of the trace elements the Rh tube was operated at 60 kV and 45 mA. LiF(200) crystal and 100 $\mu$  collimator were used throughout. The detector for Ba and La was the gas-flow proportional counter, and for V, Cr and Ce this counter was used in tandem with the sealed Xe counter. A scintillation counter was used for the rest of the trace elements. A total of 44 international silicate rock reference materials, with compositions ranging from basaltic to rhyolitic, were used for the calibrations (Govindaraju 1994, 1995). For the major elements the fundamental parameter (FP) matrix correction model in the SuperQ software was used. For Ni, Cu, Zn, Rb, Sr, Y, Zr, Nb, Pb, Th and U the mass attenuation corrections are based on measuring the intensity of the Compton K<sub>K</sub> line of Rh. For Ba, La, Ce, V and Cr determination of the major elements were included and the FP matrix correction model was used. The analyses are presented in Table 1.

### Major element geochemistry Comparison with similar rock-types

In addition to the field association with obvious metasedimentary rocks, the major element chemistry should be able to provide some evidence for the provenance of the sillimanite-bearing rocks. Firstly, these sillimanite schists and

gneisses seem to be roughly similar to the so-called kinzigites in Finland, rocks which Simonen (1953) concluded were originally argillaceous sediments. Comparison with main element trends from the Rønne kaolinite on Bornholm (Bondam 1967) also shows that the South Norwegian sillimanite schists may have had clay-dominated sediments as precursors.

### Plotting in a classification system for argillaceous rocks

In a worldwide study of argillaceous rocks, Englund & Jørgensen (1973b) established a triangular weathering trend diagram (Fig. 2). According to these authors the most unweathered sediments plot in field A II in the triangular diagram (see Fig. 2). Increased weathering will move them

downwards to fields A III or B III, and successively to A IV, B IV and finally into field C IV as alumina-rich rocks. This trend is the result of gradual progressive chemical weathering, leading to increasing maturity of the sediments. This evolution may also be expressed by the following two equations:

$$1) \quad M_1 = \frac{\text{FeO} + \text{MgO} + \text{Al}_2\text{O}_3}{\text{K}_2\text{O} + \text{Na}_2\text{O} + \text{CaO}}$$

$$2) \quad M_2 = \frac{\text{Al}_2\text{O}_3}{\text{FeO} + \text{MgO}}$$

As the concentrations of these elements change during progressive weathering, the ratios in the above formulas will differ in a certain pattern. Passing from unweathered sediments to increasingly more weathered rocks,  $M_1$  will gradu-

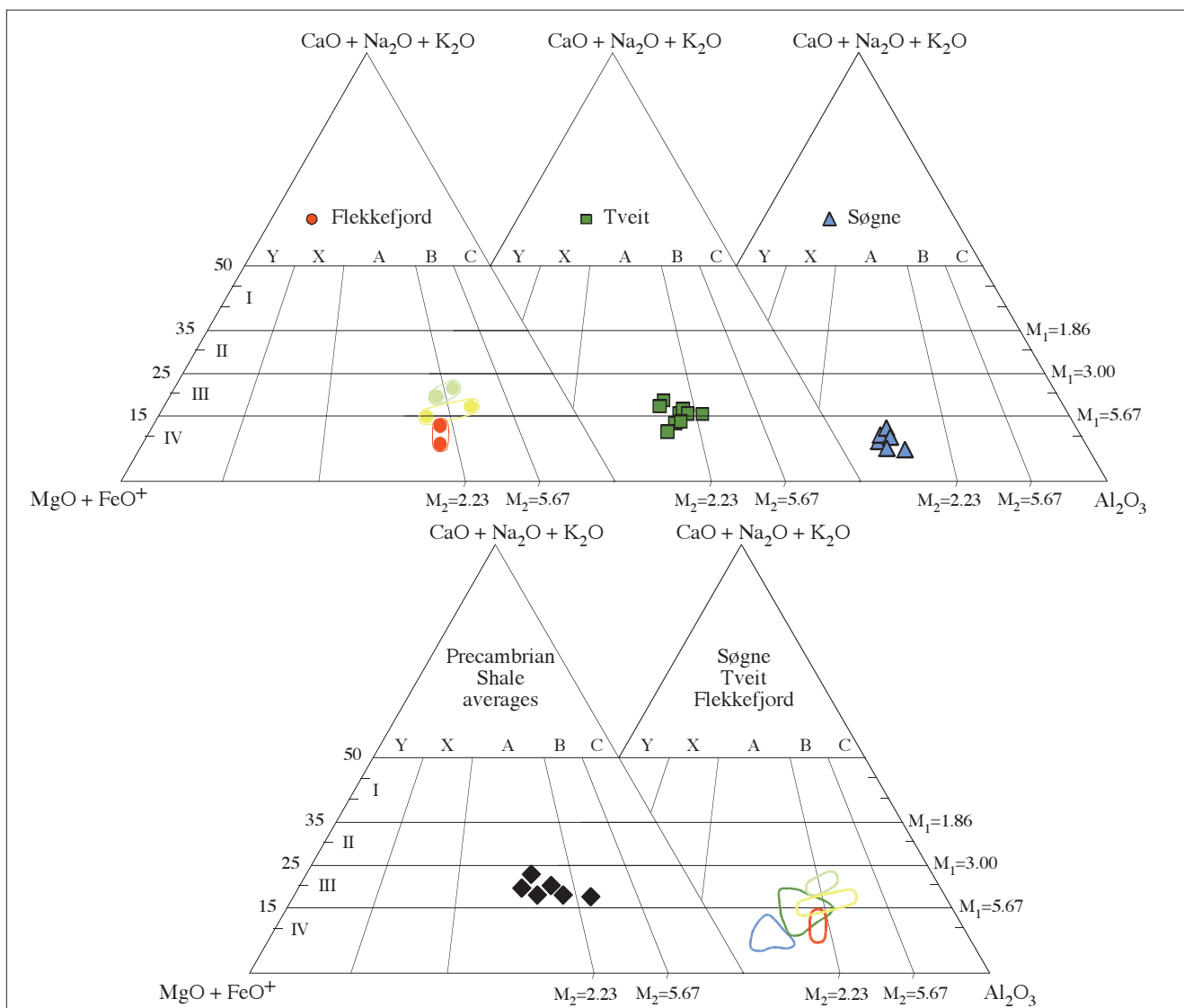


Fig. 2. Weathering trend diagram from Englund & Jørgensen (1973b). Gradual increase in weathering, resulting in loss of Ca, Na and K, is shown by an increase in  $M_1$  (Fields I to IV). Extreme weathering is shown by an increase in  $M_2$  (Fields A IV to C IV). The Søgne schists (blue triangles) and the Flekkefjord schists (red filled circles) are accordingly slightly more weathered than the Tveit schists (green squares) and the quartz-rich sillimanite gneisses (yellow filled circles). The felsic sillimanite gneisses (pale green filled circles) from the Flekkefjord area are apparently the least weathered. The black diamonds are Precambrian pelites and schists from North America, Brazil, Australia and Russia (Cameron & Garrels 1980, Condie 1993, Gromet et al. 1984, Herz 1962, McLennan 1989, Ronov & Migdisov, 1971, Taylor & McLennan, 1985).

ally increase, whereas  $M_2$  will remain essentially constant (Englund & Jørgensen 1973b). During advanced chemical weathering,  $M_2$  will increase rapidly whereas  $M_1$  will remain almost constant, resulting in an alumina-rich sediment ending with aluminous bauxite. They recognised that the chemical composition of the source rock affects the weathering trend, and rocks with basic compositions may under certain conditions move towards the FeO + MgO corner in the diagram and end up as ferric laterite.

Plotting our analyses in Fig. 2, the *Flekkefjord biotite-garnet-sillimanite schists* plot in the A IV field, indicating a highly weathered precursor. The *quartz-sillimanite gneisses* plot low in the A III and B III fields, suggesting slightly less weathered precursors, whereas the *felsic sillimanite gneisses* plot higher in the same fields indicating still less weathering. The *Tveit schists* plot slightly above the *Flekkefjord schists*, whereas the *Søgne schists* plot below these in the lower part of the A IV field, slightly shifted towards the iron/magnesium corner (Fig. 2).

The  $M_1$  values show large variations from 3 to almost 12, whereas there is little variation in  $M_2$  (Fig. 3, Table 1). The *Søgne schists* have the highest  $M_1$  values (9–12), together with one of the *Flekkefjord schists*. The other *Flekkefjord schist* has a value of 7, together with the most weathered *Tveit schist*. The rest of the *Tveit* samples have  $M_1$  values between 4.5 and 6.5, similar to the quartz-sillimanite gneisses. The felsic sillimanite gneisses have values below 5, similar to Precambrian shales and pelites from other parts of the world. The higher the  $Al_2O_3$  content in the sillimanite schists, the higher is the MgO + FeO content, thus preventing an increase in  $M_2$ .

Judging by the major element distribution in Figs. 2 & 3, the sillimanite rocks resemble highly weathered material of sedimentary origin. Their precursors are distinctly different from the Pleistocene glacial clays and are obviously more weathered than the Neoproterozoic and Cambro-Ordovician successions in south central Norway (see plots in Englund & Jørgensen 1973a). However, the precursors did not develop as far as converting into either bauxite or laterite.

### Comparison with Precambrian low-metamorphic lutites

The chemical variation of the sedimentary lutite or argillite group is controlled by the varying ability of different minerals to resist weathering. As plagioclase is one of the first minerals to decompose, calcium and sodium will decrease rapidly if the dissolved material is removed from the sediment. Under more intense weathering conditions, K-feldspar and ferromagnesian minerals will also dissolve with loss of their constituents, apart from those elements that are included in the resulting hydrous aluminium and/or ferrous silicate minerals.

Nesbitt & Young (1982) investigated the weathering conditions of ancient sediments of the lutite group in the Palaeoproterozoic Huronian Supergroup in Canada. This is a 12 km-thick succession of sedimentary and volcanic rocks

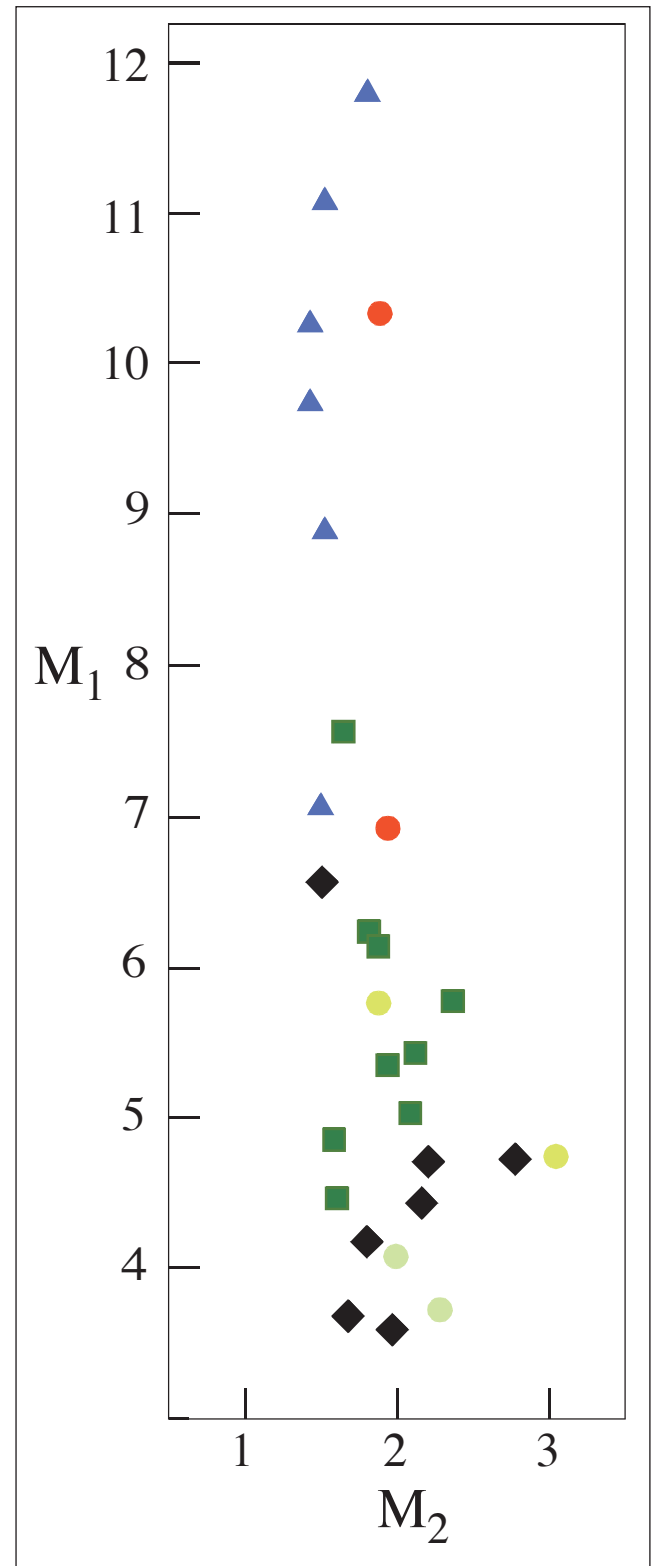


Fig. 3. The  $M_1$ - $M_2$  functions (Englund & Jørgensen 1973b) illustrate a supposed increase in weathering. The *Søgne biotite-garnet-sillimanite schists* and the *Flekkefjord biotite-garnet-sillimanite schists* appear to be the most weathered. The symbols are the same as in Fig. 2.

Table 1. Analyses of the biotite-garnet-sillimanite schists, the quartz-sillimanite gneisses (Q30-3, Q29-12) and felsic garnet-sillimanite gneisses (A24-27, A24-29). All analyses are recalculated to 100 wt% on a volatile-free basis.

	TVEIT										SØGNE										FLEKKEFJORD										PAAS		APCS	
	G25-5	G25-7	G25-8	G25-9	G25-10	G25-11	G25-12	K23-17A	K23-17B	OFT-1	OFT-2	OFT-3	OFT-4	O19-50A	O19-50B	A24-6	A24-31	Q30-3	Q29-12	A24-27	A24-29	PAAS	APCS	PAAS	APCS									
SiO <sub>2</sub>	55.40	58.00	56.50	59.85	59.10	59.22	62.05	58.29	58.70	43.63	39.78	39.36	40.11	39.65	38.62	46.39	47.70	65.55	74.77	55.37	57.42	64.17	66.17	64.17	66.17									
TiO <sub>2</sub>	1.20	1.15	1.30	0.97	1.01	1.03	0.80	1.34	1.30	1.39	1.64	1.49	1.50	1.50	1.68	1.47	1.55	1.20	0.84	0.99	0.96	1.02	0.68	1.02	0.68									
Al <sub>2</sub> O <sub>3</sub>	24.32	22.68	23.17	21.76	22.85	22.22	22.28	20.50	20.13	28.45	31.74	34.84	31.06	31.40	32.60	30.05	30.26	20.32	13.50	23.19	22.72	19.31	18.5	19.31	18.5									
Fe <sub>2</sub> O <sub>3</sub>	0.08	0.52	0.08	0.42	0.46	0.62	0.00	0.18	0.21	0.79	0.84	1.71	1.40	1.17	0.95	1.04	1.16	0.77	0.28	1.12	0.89													
FeO	8.71	8.93	10.50	8.18	7.70	8.57	6.82	9.62	9.38	13.02	14.42	12.83	15.03	15.52	15.68	10.74	11.07	4.63	5.54	8.21	6.94	6.64	5.97	6.64	5.97									
Mn <sub>3</sub> O <sub>4</sub>	0.16	0.12	0.12	0.10	0.08	0.10	0.08	0.10	0.10	0.27	0.27	0.28	0.35	0.34	0.33	0.11	0.15	0.04	0.11	0.11	0.09	0.11	0.11	0.11	0.11									
MgO	2.90	2.63	3.38	2.52	2.58	2.70	2.45	3.06	2.83	4.73	5.41	4.88	5.13	5.21	5.22	3.61	3.62	1.35	1.34	2.38	2.16	2.25	2.33	2.25	2.33									
CaO	1.51	0.58	0.77	0.71	0.73	0.70	0.45	0.84	1.08	1.83	0.65	0.44	0.76	0.65	0.46	0.62	0.40	0.90	0.57	0.96	1.04	1.33	0.75	1.33	0.75									
Na <sub>2</sub> O	2.22	0.91	0.99	1.14	1.24	1.10	0.81	1.35	1.70	2.10	0.70	0.43	0.87	0.71	0.45	1.22	0.92	0.92	0.78	2.35	2.63	1.23	1.12	1.23	1.12									
K <sub>2</sub> O	3.42	4.13	3.16	4.30	4.20	3.69	4.21	4.65	4.48	3.76	4.52	3.72	3.76	3.62	3.99	4.71	3.13	3.86	2.23	5.25	5.07	3.78	3.83	3.78	3.83									
P <sub>2</sub> O <sub>5</sub>	0.08	0.05	0.03	0.05	0.05	0.05	0.07	0.08	0.08	0.03	0.03	0.02	0.03	0.02	0.02	0.04	0.04	0.46	0.04	0.07	0.08	0.16	0.13	0.16	0.13									
Nb	31	19	24	18	16	16	18	18	17	18	20	17	19	20	21	29	35	21	19	20	19	19	19	19	19									
Zr	230	201	216	161	173	164	184	229	224	205	223	255	237	244	236	306	299	351	382	226	246	210	196	210	196									
Th										5	8	6	6	9	9	23	23	27	24	24	24	15	14	15	14									
Ce	59	45	56	38	47	47	59	57	55	26	16	17	20	24	17	88	98	109	79	142	214	80	82	80	82									
La	56	33	17	27	36	36	29	27	27	81	80	76	98	104	98	65	54	42	63	62	58	27	35	27	35									
Sr	127	90	55	119	114	93	93	98	119	419	136	98	184	143	4	49	57	59	34	57	109	38	38	38	38									
Ba	493	692	381	827	756	646	791	914	863	671	799	764	742	1053	1060	1054	638	351	170	1579	1521	200	108	200	108									
Rb	217	239	229	220	220	212	204	284	271	239	284	245	252	252	258	189	112	126	88	156	151	160	165	160	165									
V	172	218	257	195	202	206	124	212	205	254	322	315	284	331	348	255	252	273	117	148	130	150	100	150	100									
Cr	96	115	130	108	101	105	73	110	100	161	196	213	197	206	232	288	173	322	95	81	110	115	110	115	110									
Ni	38	42	49	38	35	41	30	43	42	55	67	78	87	96	89	69	61	40	21	51	47	55	52	55	52									
M1	5.06	6.23	7.56	5.34	5.44	6.20	5.77	4.87	4.47	7.06	8.92	11.78	9.74	10.27	11.07	6.92	10.33	4.75	5.76	4.06	3.73	4.45	4.7	4.45	4.7									
M2	2.08	1.84	1.65	1.86	2.14	1.88	2.4	1.60	1.62	1.51	1.54	1.81	1.45	1.44	1.51	1.87	1.92	3.05	1.89	3.73	2.29	2.17	2.23	2.17	2.23									
CIA	71	76	78	74	74	76	77	70	68	71	81	86	82	83	85	79	84	74	74	67	66	69	69	69	66									
Fe/Mn	59	85	146	128	109	137	92	147	143	55	61	55	50	53	54	115	87	144	57	90	93	59	59	59	59									
Zr/Nb	7.4	10.5	9.0	8.9	10.8	10.3	10.2	12.7	13.2	11.4	11.2	15	12.5	12.2	11.2	10.6	8.5	16.7	20.1	11.3	12.9	11.1	11.7	11.1	11.7									
Zr/Y	3.9	4.5	3.9	3.2	4.6	3.5	4.8	5.6	5.1	2.5	2.8	3.4	2.4	2.3	2.4	4.7	5.5	8.4	6.1	3.6	4.2	7.8	5.6	7.8	5.6									
Ce/La	1.8	1.8	1.9	2.1	1.9	1.8	2.0	2.1	2.0	1.3	1.1	1.7	1.8	1.8	1.7	2.0	1.7	1.8	2.3	2.1	2.0	2.1	2.1	2.1	2.1									
Ce/Y	1.7	1.3	0.6	1.1	1.8	1.4	1.6	1.4	1.3	0.3	0.2	0.2	0.2	0.2	0.2	1.5	1.8	2.6	1.3	2.3	3.7	3	3	3										
Cr/Ni	2.5	2.7	2.7	2.8	2.9	2.6	2.4	2.6	2.4	2.9	2.9	2.7	2.3	2.1	2.6	4.2	2.8	8.1	18.2	1.9	1.7	2	2	2	2									

that were deposited between 2.5 and 2.1 Ga ago. As aluminium increases and calcium and the alkalis decrease with progressive weathering, a good measure of the degree of weathering may be obtained from the major element chemistry by their so-called chemical index of alteration (CIA) (Nesbitt & Young 1982, p.715). The CIA is obtained from the following formula using molecular proportions:

$$\text{CIA} = (\text{Al}_2\text{O}_3 / (\text{Al}_2\text{O}_3 + \text{CaO} + \text{Na}_2\text{O} + \text{K}_2\text{O})) \times 100$$

The CaO is the amount of this oxide in the silicate fraction and should be corrected for any carbonate or apatite content. As carbonates are absent and the amount of apatite is negligible in our samples (apart from Q30-3), such a correction was inappropriate in this particular case.

As pointed out by Nesbitt & Young (1982), CIA values for average shales range from about 70 to 75 due to a large proportion of hydrous aluminium silicates and related minerals. The Elsie Mountain and McKim formations in the Huronian Supergroup have CIA values between 64 and 87 (average 81) and between 67 and 86 (average 75), respectively. On the basis of these results it was concluded that the sediments derived from highly weathered detritus and that the CIA was "suggestive of weathering in humid, possibly tropical conditions" (Nesbitt & Young 1982).

The 21 samples from southern Norway have CIA values between 66 and 86 (average 76) and are thus comparable to the McKim formation (TABLE 1). The *Søgne* samples range between 71 and 86 (average 81), comparable to the highly weathered Elsie Mountain formation. Omitting Oft-1 (CIA=71), the five remaining samples vary between 81 and 86 (average 83), indicating a highly weathered precursor that formed in a warm, humid climate.

The *Flekkefjord schists* have an average CIA index of 82 (79 to 84) whereas the *quartz-rich gneisses* have values of 74. The *felsic sillimanite gneisses* have values of 66 and 67. Accordingly, the schists probably had a highly weathered precursor, whereas the felsic sillimanite gneisses were derived from less weathered material. The quartz-rich gneisses also seem to be derived from highly weathered precursors.

In the main *Tveit* profile, except for sample G25-6 (CIA = 71) the remaining six samples range between 74 and 78 (average 76). The two samples from *Gill* have CIA values of 68 and 70, which place them among the moderately weathered shales.

The two felsic gneisses from Flekkefjord have weight%  $\text{Al}_2\text{O}_3 / (\text{CaO} + \text{Na}_2\text{O})$  ratios below 10, which is also the case for the two border samples and the Gill samples, whereas the rest of the population have ratios between 11 and 40 (Fig. 4). The high ratios indicate highly weathered precursors. The CIA average value for the whole population of 21 samples is 76, and for the 15 samples without a pronounced alkali content the CIA is 79. According to Nesbitt & Young (1982) the high ratios in this study preclude glacial sediments as precursors, but indicate aggressive weathering under humid, warm conditions, possibly in a tropical climate.

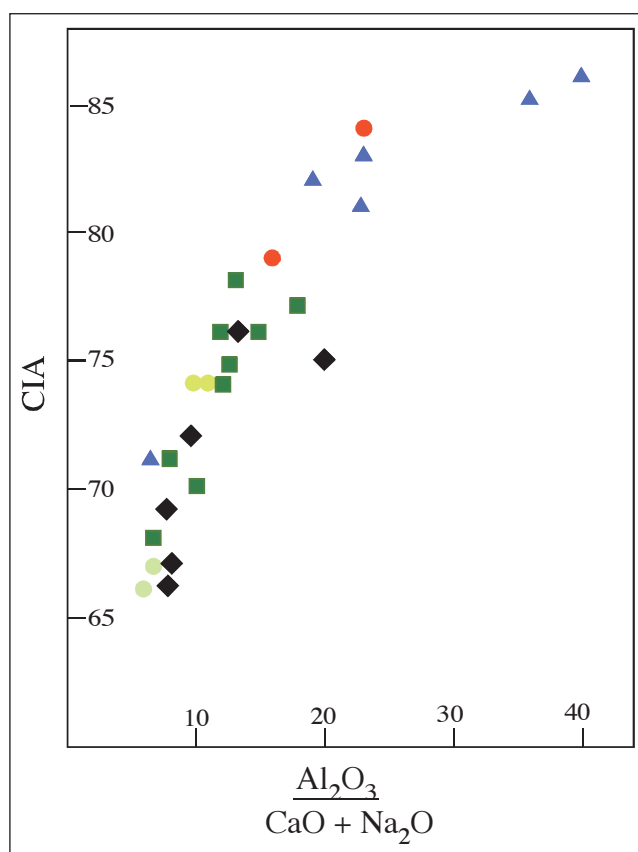


Fig. 4. The CIA index (Nesbitt & Young 1982) versus weight%  $\text{Al}_2\text{O}_3/(\text{CaO} + \text{Na}_2\text{O})$  showing that the Søgne and the Flekkefjord biotite-garnet-sillimanite schists are more weathered than the Tveit schists and the sillimanite-bearing gneisses from Flekkefjord. Symbols as in Fig. 2.

### Chemical weathering trends

Nesbitt & Young (1989) found that weathering trends could be displayed on a  $(\text{CaO} + \text{Na}_2\text{O}) - \text{Al}_2\text{O}_3 - \text{K}_2\text{O}$  triangular diagram (Fig. 5). The population from southern Norway apparently follows a trend parallel to and intermediate between the weathering trends for Average gabbro and Average granite (Fig. 5). Plutonic rocks such as monzonites, diorites and tonalites, or their volcanic counterparts, presumably follow intermediate weathering trends.

The samples plot neither close to the unweathered rocks nor near the relatively little weathered part of the diagram, which is consistent with the previous indications that the most alumina-rich samples were originally highly weathered clay-rich rocks. The least alumina-rich samples plot close to the field for the average Precambrian pelite/shale composition (Fig. 5). The Søgne schists plot towards the most weathered part, between the end products of gabbro and granite. These sillimanite-bearing rocks are evidently more alumina-rich and depleted in calcium and sodium than the average Proterozoic pelitic shales.

### Sedimentary processes

The previous plots support a metasedimentary provenance, but it is important to emphasize the compositional complexity of sedimentary rocks as there are at least four main

factors which have to be considered. Chemical weathering in situ or during transport may cause profound alteration of the provenance rock(s) and judging from the previous plots this has obviously been an important factor. The source rock in the provenance area is also important; if there are several source rocks, a mixing of the debris or weathered material may cause different chemical trends. Other processes during sediment transport and deposition, such as grain-size sorting, adsorption and other syn- or post-depositional alterations may change the geochemical signature of the provenance rocks profoundly. Moreover, diagenesis and metamorphism may also cause element mobility. Unfortunately, the nature of the source rock is unknown. All the country rocks, except the other metasediments, are seemingly younger, leaving the metasedimentary complex as relics in a multitude of later intrusions.

$\text{TiO}_2$ ,  $\text{FeO}_T$  and  $\text{MgO}$  are mostly derived from the mafic minerals and retained in clay minerals. The high values and linear relationship between these elements indicate that the sillimanite-bearing schists have been derived from mafic source rocks (Table 1). Furthermore, the higher concentrations of these elements in the Søgne schists indicates that they were derived from more mafic source rocks than the Flekkefjord-Tveit schists. The quartz-rich gneisses may have been derived from more felsic rocks unless processes such as reworking, mixing and sorting have occurred. Grain-size sorting may concentrate quartz and perhaps some alkali feldspar together with other resistant minerals in the sand fraction, whereas most of the mafic elements will be concentrated in the clay fraction. Silica will normally be concentrated in the coarse fraction due to grain-size sorting. There is a rather irregular increase in silica with decreasing  $\text{TiO}_2$  which indicate that several processes may have acted together (Table 1). Alumina shows the opposite relation, explained by its important role in clay minerals, and grain-size sorting may have concentrated the most fine-grained material in the Søgne and Flekkefjord schists, whereas the Tveit schists and the gneisses all have had a lower clay content. The trend of the quartz-rich samples overlap with those from a turbidite sequence in New Zealand (Korsch et al. 1993) but this does not necessarily imply that these rocks have been turbidites, but suggests that grain-size sorting may have been active. The irregular trends of the other major elements suggest that weathering played a major role in their formation.

### Trace element geochemistry Trace element distribution of lithophile elements

In a relatively wet climate, hydrous solutions are expected to play an important role in dissolving minerals and controlling the behaviour of elements during transportation and precipitation. Important in this connection is the *Ionic Potential* (IP) or *Field Strength* (FS) which is defined as  $Z/r$ , where  $Z$  is the ionic charge and  $r$  the ionic radius. This factor will, to some extent, control the solution/precipitation behaviour of

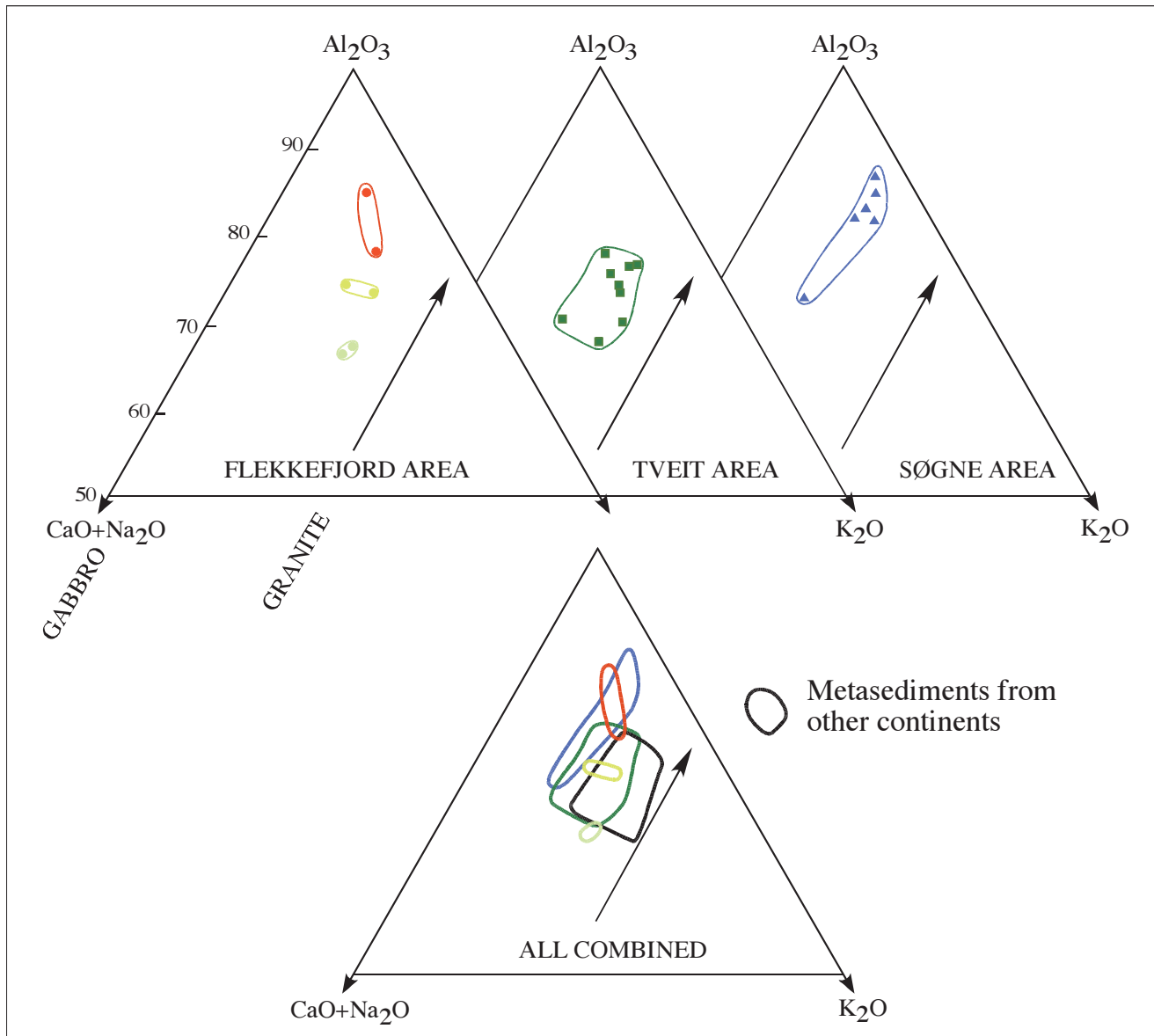


Fig. 5. Samples from the Flekkefjord, Tveit and Søgne areas plotted on the chemical trend diagram of Nesbitt & Young (1989). The average gabbros plots along the left side of the triangular diagram from about 50 to 40%  $\text{Al}_2\text{O}_3$ . The average granite plots at the lower end of the central arrow. Symbols as in Fig. 2.

the different elements. Elements with an ionic potential or field strength less than 2 (denoted LFSE or Low Field Strength Elements) will be easily dissolved. Thus, Sr, Ba, K and Rb will be removed in hydrous fluids as soluble cations during weathering and remain in solution during transportation. Elements with higher Field Strength (or HFSE with FS between 2.5 and 9.5) (Krauskopf & Bird 1995) become fixed to hydroxyl groups and are precipitated by hydrolysis. Elements with FS higher than approximately 10 or 11 will normally form soluble anionic complexes. In the present investigation this includes phosphorus (P). Spider diagrams in this study are constructed with P (highest FS) on the left followed by elements with gradually decreasing FS values (Figs. 6-11).

The pH and redox potential also influence the element distribution during sedimentary processes. Colloidal

processes, where sols and gels influence precipitation, may be an important factor, such as the adsorption of K, Rb and Ba to montmorillonite-rich clay. Some heavy metals, such as V, may also be adsorbed under certain conditions and thus be removed from solution by natural colloids.

Despite these complications, which may influence the element distribution, an attempt to identify the nature of the protolith has been made by normalising all the analysed trace elements to different average estimations such as Average Proterozoic Cratonic Shale (APCS) (Condie 1993) or Post Archaean Australian Shale (PAAS) (McLennan 1989). PAAS is applied in Figs. 6-14 and APCS in Fig. 15.

All samples, with just one exception (one of the *quartz-sillimanite gneisses*, Q30-3), have pronounced negative P anomalies in the spider diagrams. The positive anomaly for P in Q30-3 ( $\text{P}_2\text{O}_5 = 0.46\%$ , PAAS 0.16%) is unique and the high



Fig. 6. The elements of the quartz-rich sillimanite gneisses from the Flekkefjord area normalised to the composition of PAAS (Post-Archaean Australian Shale; McLennan 1989). The elements are in succession with decreasing ionic potential towards the right.

abundances of Zr, Th, Ce, La and Y may be due to the presence of zircon, monazite and/or xenotime in the sand fraction (Fig. 6). The other relatively quartz-rich gneiss (Q29-12) has an even higher Zr content. Both samples have negative anomalies for Sr, Ba, K and Rb.

The felsic garnet-sillimanite gneisses possess positive anomalies for Ce, Y, La, Ba and K; otherwise the concentrations of Nb and Ti are equivalent to PAAS, whereas Zr is only slightly positive (Fig. 7). The generally high enrichment ratios in the biotite-garnet-sillimanite schists from the Flekkefjord area include a pronounced positive anomaly for Y with an enrichment factor of two or more, which is also the case for the most quartz-rich gneiss (Fig. 8).

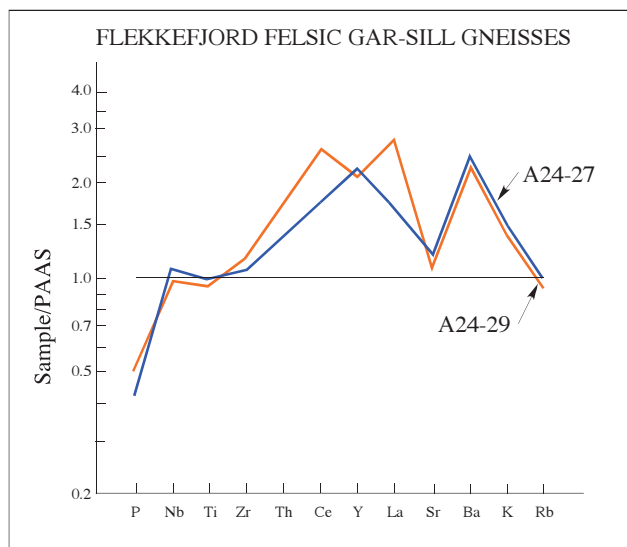


Fig. 7. The felsic garnet-sillimanite gneisses from the Flekkefjord area normalised to PAAS.

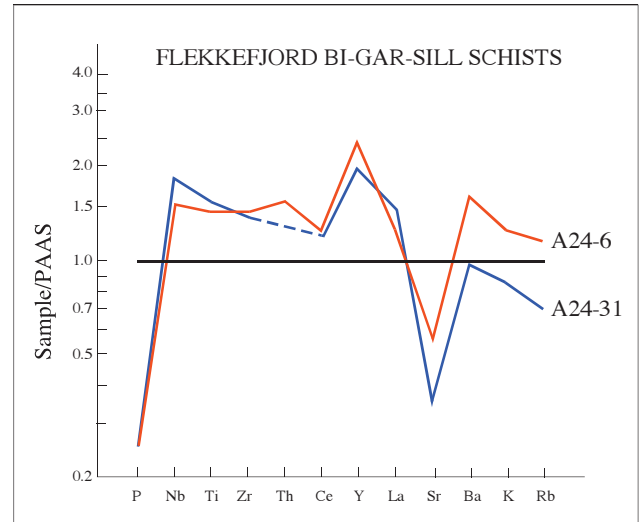


Fig. 8. The Flekkefjord biotite-garnet-sillimanite schists normalised to PAAS.

The spider diagram for the *Tveit schists* is shown in Fig. 9 and for the *Søgne schists* in Fig. 10, where Y in particular shows large positive anomalies (Fig. 11). On the other hand, Ce and La exhibit large negative anomalies.

The low field strength elements (LFSE) or large-ion lithophile elements (LILE) Sr, Ba, K and Rb also vary with rock type and area. Sr in particular shows large negative anomalies. All rocks have positive Ba anomalies, except the quartz-rich gneisses. K is also enriched relative to PAAS, except in the most quartz-rich gneiss. Almost all *Flekkefjord rocks* have negative Rb anomalies, as opposed to distinct positive enrichment ratios in the *Tveit* and *Søgne schists*.

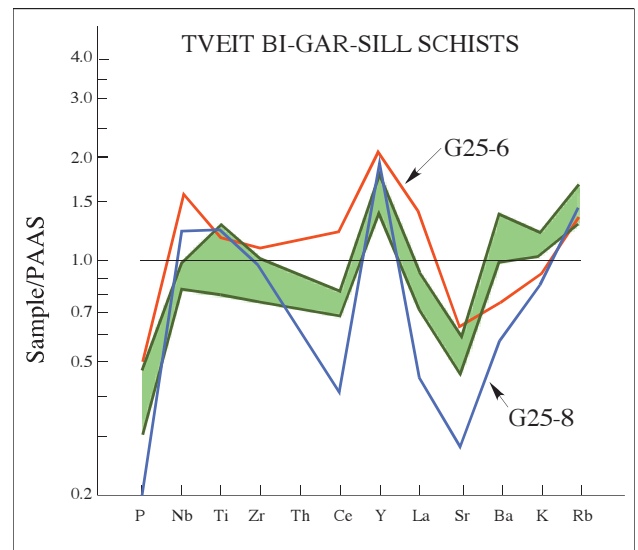


Fig. 9. The Tveit biotite-garnet-sillimanite schists normalised to PAAS. The red curve is the border sample (G25-6) and the blue curve is the ferromagnesian rich sample (G25-8). The seven other samples lie within the green band.



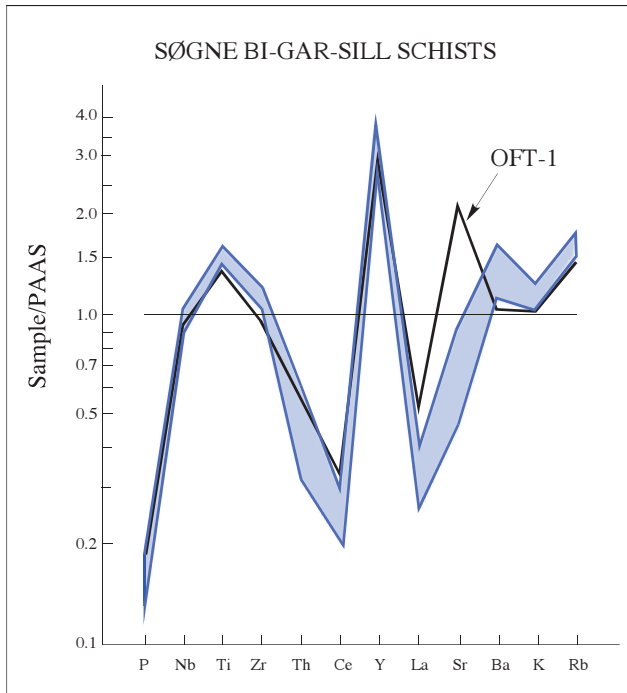


Fig. 10. The Søgne biotite-garnet-sillimanite schists normalised to PAAS. Five samples are within the blue band and the black curve is the border sample (Oft-1).

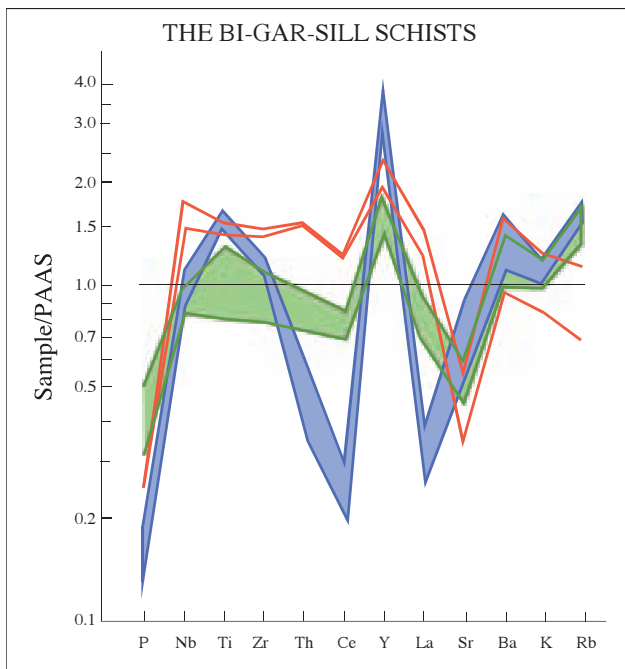


Fig. 11. The red curves are the Flekkefjord biotite-garnet-sillimanite schists; the blue belt contains the Søgne biotite-garnet-sillimanite schists (minus the border sample). The green area covers seven Tveit biotite-garnet-sillimanite schists (excluding G25-6 and G25-8).

### The transition elements

The plots are arranged according to the position of the elements in the periodic table. All samples are normalised against the PAAS (McLennan 1989) and the APCS (Condie 1993).

The *quartz-rich gneisses* have positive Cr anomalies and negative Mn, Fe and Ni anomalies (Fig. 12B). The most quartz-rich gneiss also shows negative Ti and V anomalies. The other quartz-rich gneiss has a similar trend to the biotite-garnet-sillimanite schists (Fig. 12A,B), although distinctly lower in Mn, Fe and Ni.

The *felsic garnet-sillimanite gneisses* are relatively depleted for most transition elements, apart from slightly higher Fe contents. This is presumably largely situated in the garnets and to a lesser extent in the small amount of biotite (Fig. 12C,D).

The *Flekkefjord schists* occupy an intermediate position below the Søgne schists and above the Tveit and Gill schists (Figs. 12D, 13A-D, 14A-C, 15D). The *biotite-garnet-sillimanite-schists* from Søgne (Fig. 14A,B) show the highest positive anomalies, except for Cr (Fig. 12A,B, 14C, 15C). Mn is enriched in the Søgne schists, unlike the other schists. The high V enrichment is important, since V may signal the presence of adsorption to clay minerals, in a similar manner to Ba, K and Rb.

### Discussion

The composition of the atmosphere during the Proterozoic was depleted in oxygen and Precambrian sediments in general differ from modern types as a result of environmental differences (Ronov & Migdisov 1971, Condie 1993). Generally, there seems to be less Na<sub>2</sub>O and CaO in many Precambrian sedimentary rocks, probably because of more intensive weathering and/or extensive recycling. Plagioclase is one of the first minerals to be attacked during aggressive weathering. Possibly due to the effect of acid rain on the vegetation-free rocks during the Proterozoic, both Na and Ca may have been efficiently removed in solution. Condie (1993) showed that Na, Ca, Sr and Ba were deficient in shale/sandstone mixtures relative to upper crustal sources throughout the Precambrian, whereas Fe and Ti were in excess in Archaean sediments. With these precautions in mind, the behaviour of the analysed elements is discussed below.

*Phosphorus* is a normal constituent of many sedimentary environments. The strong negative anomalies for almost all the sillimanite-bearing rocks may indicate that it stayed in solution in the form of soluble anion complexes during formation of the precursors to the sillimanite rocks. Alternatively, phosphorus may have been dissolved and removed during diagenesis or, less likely, during metamorphism.

*Niobium* in most of the sillimanite-bearing rocks seems to be in the normal range (16-24 ppm Nb), apart from the Flekkefjord biotite-sillimanite schists and the Tveit border sample which have higher values (29-35 ppm Nb versus 19

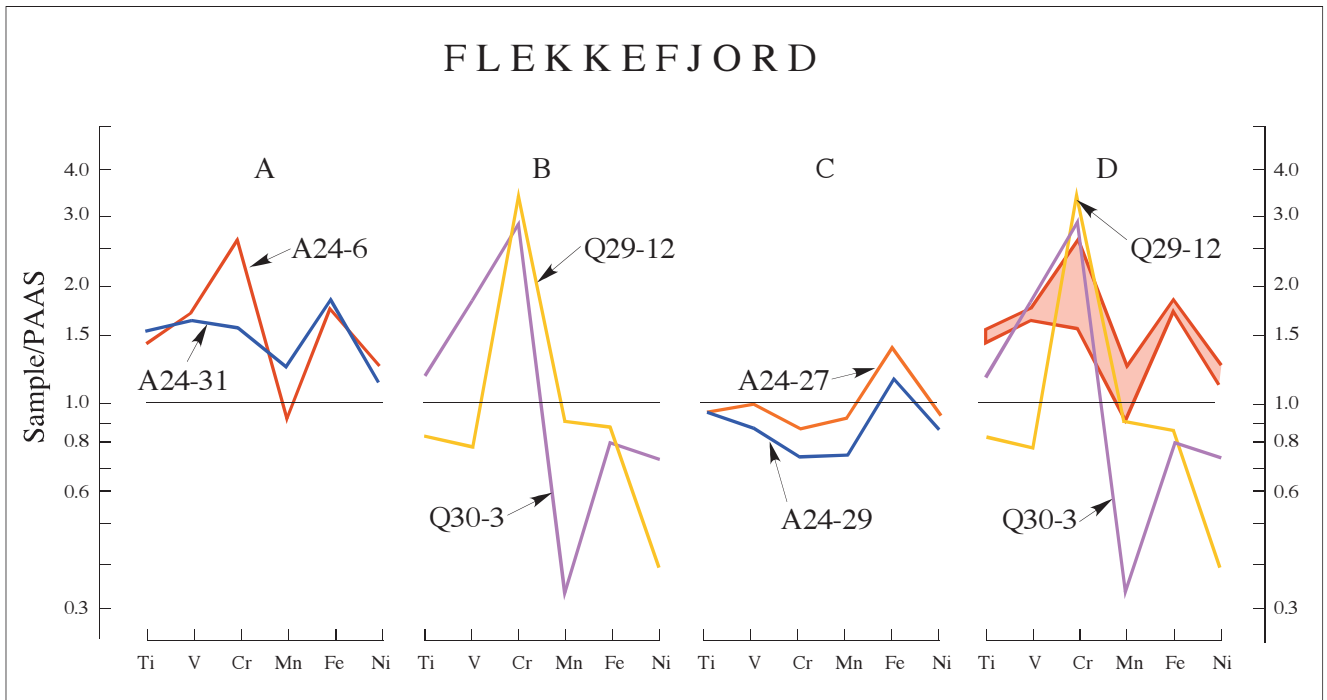


Fig. 12. The Flekkefjord biotite-garnet-sillimanite schists and sillimanite-bearing gneisses normalised to PAAS. The transition elements are arranged successively according to their atomic number in the periodic table. (A) The schists. (B) The quartz-rich sillimanite gneisses. (C) The felsic sillimanite gneisses. (D) The biotite-garnet-sillimanite schists (red zone) compared with the quartz-rich sillimanite gneisses.

ppm in PAAS). Nb substitutes for Zr in zircon and the Zr/Nb ratios (Table 1) are with a few exceptions between 9 and 13 (average 11.7), compared to 11.1 and 11.7 in the PAAS and APCS, respectively. The only exceptions are the quartz-sillimanite gneisses with ratios between 17 and 20. This reflects elevated zircon contents, as their absolute Nb contents are

between 19 and 21, close to the average for all sillimanite-bearing rocks.

*Zirconium* stems from small well-rounded zircons observed in most of the samples and the Zr content in the Søgne and Tveit rocks varies between 160 and 260 ppm comparable to that in PAAS (210 ppm). There is a tendency

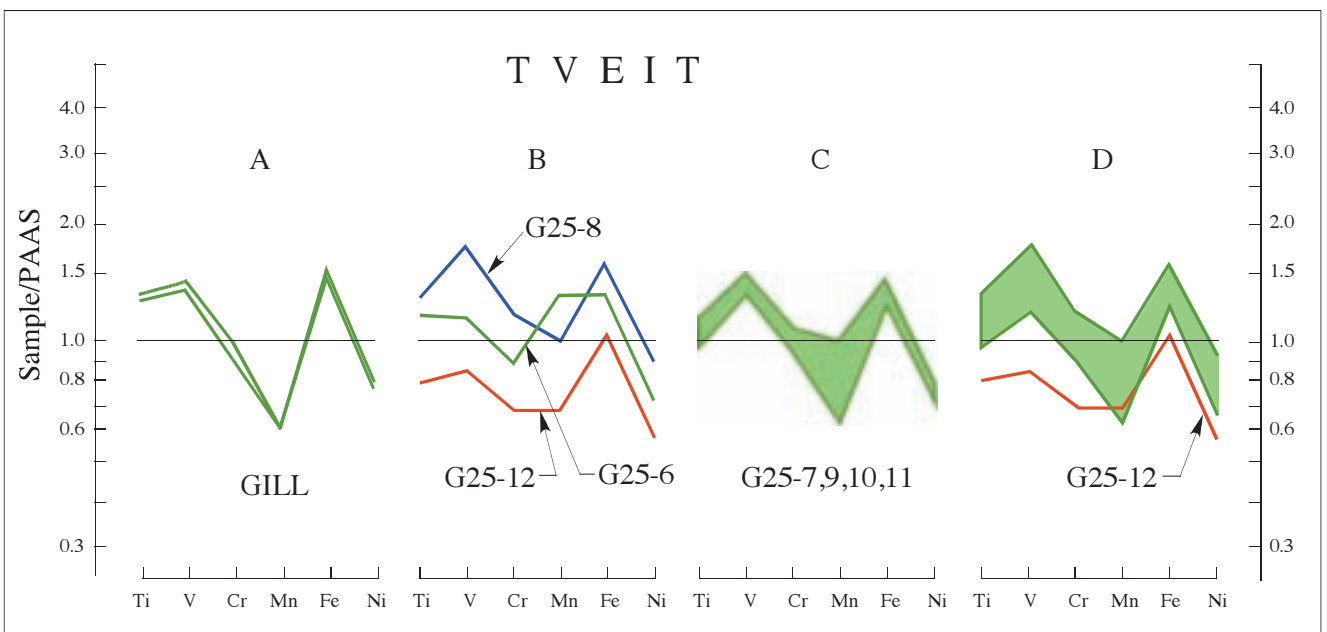


Fig. 13. The Tveit and Gill biotite-garnet-sillimanite schists normalised to PAAS. (A) The two Gill biotite-garnet-sillimanite schists. (B) The three samples with the largest deviation from the average. (C) The last four Tveit samples are contained within the green zone. (D) The green zone includes all Tveit biotite-garnet-sillimanite schists except the Mn-value of sample (G25-6). Red curve G25-12.

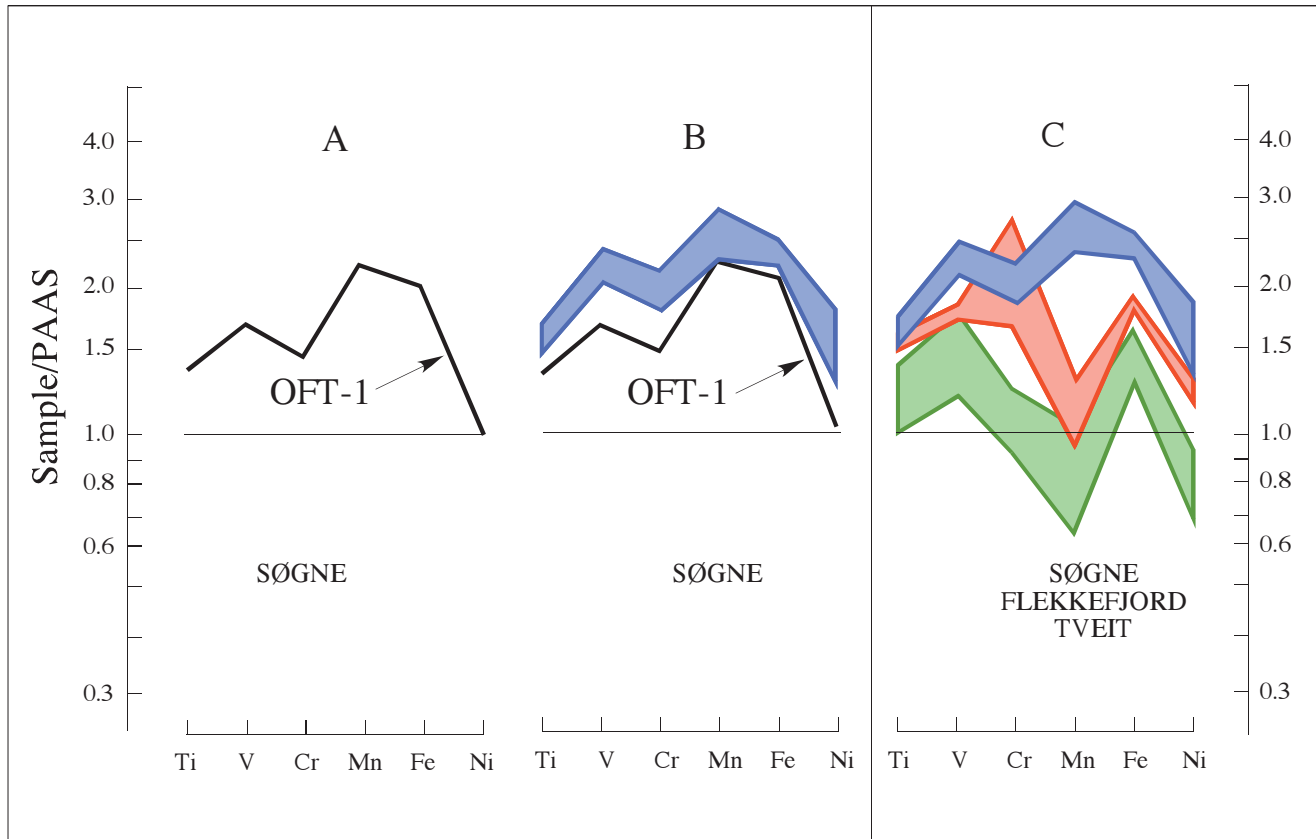


Fig. 14. The Søgne biotite-garnet-sillimanite schists normalised to PAAS. (A) The border sample (OFT-1). (B) Five Søgne biotite-garnet-sillimanite schists lie within the blue zone (OFT-1, black). (C) All biotite-garnet-sillimanite schists plotted for the purpose of comparison (Flekkefjord, red; Søgne, blue; Tveit, green).

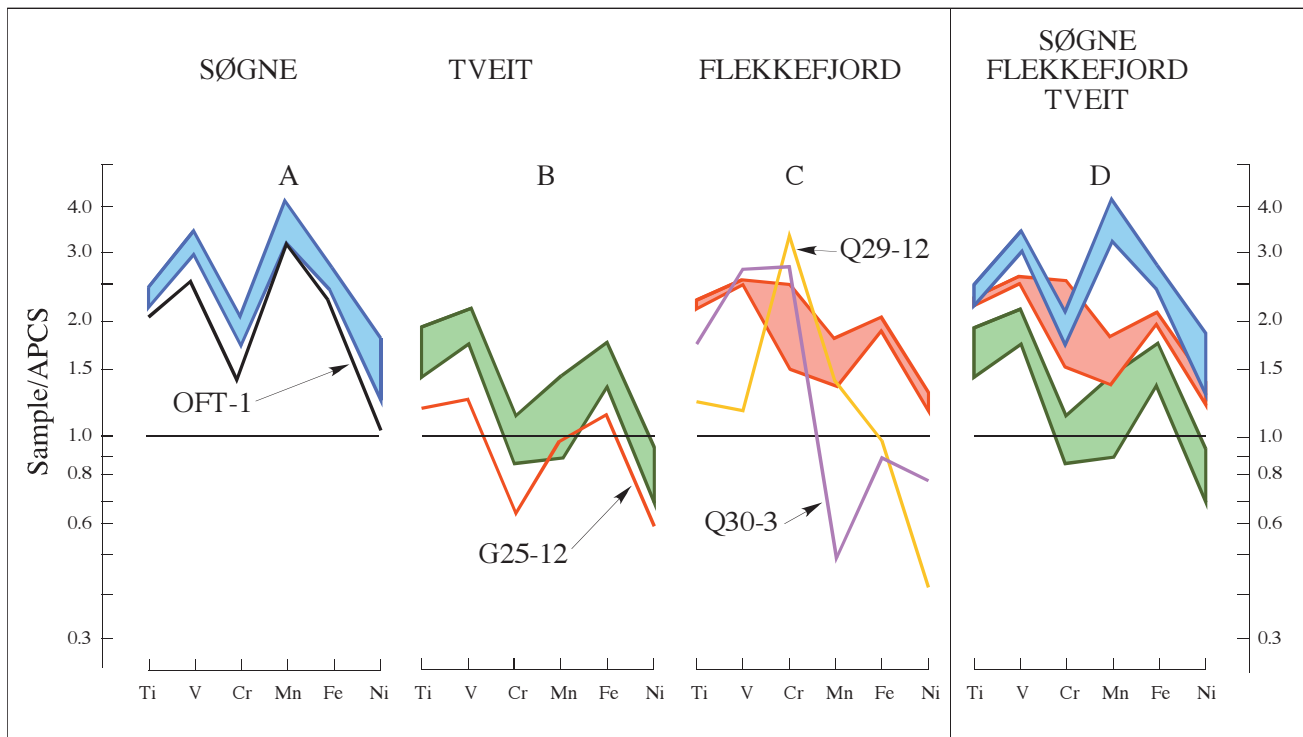


Fig. 15. All biotite-garnet-sillimanite schists and the quartz-rich sillimanite gneisses normalised to APCS (Average Proterozoic Cratonic Shale; Condie 1993). (A) The five Søgne biotite-garnet-sillimanite schists lie within the blue zone (the border sample, OFT-1, black). (B) Eight Tveit biotite-garnet-sillimanite schists lie within the green zone (G25-12, red). (C) Two Flekkefjord biotite-garnet-sillimanite schists lie within the red zone. The yellow curve (Q29-12) is for the most quartz-rich sillimanite gneiss whereas the other quartz-rich sillimanite gneiss is indicated by the purple curve (Q30-3). (D) All biotite-garnet-sillimanite schists compared (Søgne, blue; Flekkefjord, red; Tveit, green).

towards increasing Zr with increasing TiO<sub>2</sub> and a mixing processes may be able to explain this element distribution. The Flekkefjord biotite-garnet-sillimanite schists and the quartz-sillimanite gneisses have much higher values (300–382 ppm Zr). Decreasing Zr with increasing TiO<sub>2</sub> in the gneisses supports grain-size sorting.

The Zr/Y ratio (Table 1) is on average 2.6 for the Søgne schists and 4.3 for the Tveit schists, whereas the Flekkefjord schists show 5.1. The most quartz-rich gneiss has Zr/Y = 6.1 and the other quartz-rich gneiss 8.4. The PAAS-shale has a Zr/Y ratio of 7.8, whereas the APCS-shale has 5.6. As the Nb- and Zr-bearing minerals are strongly resistant to decomposition, the high values, despite the high Y concentrations, may be interpreted as the result of higher concentrations in the sand fraction in the quartz-sillimanite gneisses which have the highest positive Zr/Y values and thus support the sorting mechanism.

*Thorium* has not been analysed in all rocks and the analytical precision is poor. With some precaution it may be noted that the Flekkefjord rocks have higher values than the PAAS, whereas the Søgne schists have negative Th-enrichment ratios. The highest Th contents are found in the quartz-sillimanite gneisses, which also have the highest Zr contents, supporting the assumption of zircon enrichment.

*Cerium* is the main element in monazite, a highly resistant mineral that is chiefly derived from the weathering of granites and granite pegmatites. A regular decrease in Ce with increasing amounts of TiO<sub>2</sub> does not suggest that Ce was derived from mafic rocks. Poor analytical precision cannot be disregarded, but the large differences between the areas are probably significant. In the Flekkefjord rocks, there are small negative anomalies for both schists and quartz-rich gneisses, despite positive enrichment factors relative to PAAS. The negative anomalies in the Tveit schists are not as pronounced as those in the Søgne rocks, where the lowest enrichment factor is 0.20. On the contrary, the felsic gneisses have 142 and 214 ppm Ce, respectively, considerably above the PAAS value of 80 ppm.

Clay minerals that are precipitated in equilibrium with sea water, typically possess negative Ce anomalies (Brookins 1983, 1989, McLennan 1989). Paleo-oceanic redox conditions were studied by Wright et al. (1987) who suggested that a negative Ce anomaly indicated oxidising conditions. An Eh-pH diagram (Brookins 1989) shows a large stability field for CeO<sub>2</sub> under relatively high pH and varying oxidizing conditions. The CeO<sub>2</sub> commonly precipitates in pelagic clays with more than 100 ppm Ce and deep-sea manganese nodule deposits with over 500 ppm Ce (Li 2000). The trivalent Ce ion is stable at lower pH and positive Eh conditions and probably remains in solution during the formation of clay-dominated sediments under such conditions, thus explaining the segregation from the other trivalent lanthanides and the negative anomaly. Assuming that the precursors to the sillimanite rocks formed under prevailing hydrous conditions in a sedimentary environment, leading to precipitation of clay-rich sediments occasionally mixed with a sand fraction, the negative Ce anomalies may indicate a relatively

acid and oxidising marine depositional environment. The large negative Ce anomalies in the Søgne schists support the conclusion about strongly oxidising conditions in a marine environment, a criterion extensively used by many authors (Chen et al. 2003, McArthur & Walsh 1984, Wright et al. 1987).

*Yttrium* is a major constituent in xenotime and normally also present in monazite. Both minerals are found in granites and granitic pegmatites in southern Norway and xenotime was originally described from pegmatites in the Flekkefjord area (Berzelius 1824). All spider diagrams have distinctly positive Y anomalies. The biotite-garnet-sillimanite schists from Søgne have the highest Y anomaly and the highest value of 104 ppm Y, much higher than the 27 ppm Y in the Australian PAAS. The enrichment factors are between 2.8 and 3.9, whereas the Flekkefjord schists have enrichment ratios between 2 to 2.4 and the Tveit between 1.4 and 2.2 (Fig. 11). For all samples there is a regular decrease in Y with decreasing TiO<sub>2</sub> which mirrors the trend in Fig. 11 where Søgne values decrease gradually towards those of the Flekkefjord and Tveit schists. Surface adsorption of the lanthanides (Brookins 1989), may result in Y enrichment. Direct crystallisation of xenotime is also possible since it is isostructural with zircon, which may explain its tendency to crystallise on the surface of zircon crystals in clay deposits (Fletcher et al. 2000). McNaughton et al. (1999) conclude that "Diagenetic xenotime is common in siliciclastic rocks, where it starts to form on detrital zircon shortly after sediment deposition".

*Lanthanum* is found mainly in granitic pegmatite minerals (monazite, etc) and Ce and La commonly follow each other in many environments with a 2:1 ratio (PAAS 2.1 and APCS 2.15). The average Ce/La ratio (Table 1) increases from 1.6 in the Søgne schists to 1.9 in the Tveit and Flekkefjord schists, increasing further to 2.1 in the quartz-sillimanite gneisses and the felsic sillimanite gneisses, but the differences are probably due to poor analytical precision and are therefore not conclusive.

### The large-ion lithophile elements

Sr, Ba, K and Rb should ideally form dissolvable ions in aqueous solutions owing to their low ionic potential or field strength, unless other processes, such as adsorption, have led to their precipitation in the clay fraction.

In a sedimentary context, Sr is known from deposits formed in a dry climate. The negative Sr anomalies for all rocks but the felsic sillimanite gneisses from Flekkefjord and the Søgne border sample, may be taken as an indication that Sr was brought into solution during weathering in a humid climate and stayed in solution during formation of the precursor sediments.

*Barium* is recovered from residual clay deposits where Ba is trapped because of its higher tendency for adsorption to clay minerals than Sr. The felsic sillimanite gneisses and most of the biotite-sillimanite schists have positive Ba anomalies. Relatively high Ba in the schists may be ascribed to the adsorption model, while debris of Ba-rich feldspars may

explain the high Ba content in the felsic sillimanite gneisses. The quartz-sillimanite gneisses have negative Ba enrichment ratios, which may be explained by a relatively small fraction of clay in the sediment. In addition, the sedimentary conditions may have been unfavourable for adsorption.

*Potassium* is commonly adsorbed to clay minerals under suitable conditions. Apart from the quartz-sillimanite gneisses and one of the Flekkefjord schists, most other rocks have positive enrichment ratios. Pettijohn (1975) estimated that Precambrian and Palaeozoic shales contained on average 3.2% K<sub>2</sub>O and 1.1% Na<sub>2</sub>O, close to Condie's (1993) calculated averages for Proterozoic shales of 3.62% K<sub>2</sub>O and 1.06% Na<sub>2</sub>O compared to 3.7% K<sub>2</sub>O and 1.2% Na<sub>2</sub>O in PAAS.

In primitive Precambrian paleosoil, K was mainly derived from the weathering of K-feldspar and/or muscovite and fixed in illite, whereas Ca and Mg were dissolved and removed from the sediments. The relatively high K<sub>2</sub>O values in our samples may be explained by several processes. Diagenetic processes may give rise to some K-metasomatism (Nesbitt & Young 1989). Also, the adsorption of potassium to clay minerals leads to higher K contents. Potassium may also have been added at a later stage during metasomatism and/or magmatic injections. A variety of different processes may therefore have contributed to an increase in the K contents.

*Rubidium* occurs in small concentrations in most K-bearing minerals. The Tveit and Søgne rocks have positive Rb anomalies (204-284 ppm Rb), whereas most of the Flekkefjord samples have negative values (88-189 ppm Rb). There is a tendency towards an increase in Rb with increasing TiO<sub>2</sub> for the Søgne and Tveit schists, whereas this cannot be shown for the Flekkefjord rocks. During sedimentation dominated by clay precipitation, Rb will have a greater tendency to become adsorbed in clay minerals than K and the present distribution probably also shows the tendency for Rb to be retained by the clay minerals, since the higher the amount of clay, the higher the concentration of Rb, although this does not explain the relatively low content in the Flekkefjord schists.

The *transition elements* have intermediate ionic potentials and therefore precipitate under fluid conditions. Furthermore, precipitation from dilute hydrothermal metal-rich solutions or brines in an oceanic environment in connection with submarine volcanic activity is also possible (Gross 1980).

*Titanium-rich* minerals such as titanite, ilmenite and rutile are widely distributed in many rock-types and ilmenite is common in gabbro-norite-anorthosite complexes. During weathering, Ti may end up as extremely fine-grained anatase (TiO<sub>2</sub>) in soil deposits (Li 1991, 2000). All spider diagrams show positive or neutral Ti ratios normalised to PAAS or APCS (except one sample from Tveit, G25-12), suggesting a Ti-rich source material.

*Vanadium* is present in small quantities in many rock-types. High concentrations are found in iron-rich soils and bauxitic clays, probably due to the high degree of adsorption to clay minerals in warm, humid environments. There is

a roughly linear increase of V with increasing TiO<sub>2</sub> and FeO<sub>T</sub> (Table 1). The only exception is one of the quartz-rich gneisses, due to its lower Fe content.

The relatively high abundance of V in the biotite-garnet-sillimanite schists, especially the Søgne schists (above 3x PAAS), is in accordance with the adsorption model. The quartz-sillimanite gneiss with the highest quartz content has the lowest V content of all samples but still at a concentration between PAAS and APCS, and the gneiss with less quartz has the same amount of V as the schists, but high in relation to its FeO<sub>T</sub> and MgO contents. The felsic sillimanite gneisses have approximately the same concentrations as PAAS. This may indicate that the V contents follow the amount of clay minerals in the different rock-types and small discrepancies may be explained by different conditions during the adsorption process.

*Chromium* also shows an adsorptive tendency, which may explain the high ratios in the Flekkefjord and Søgne schists, whereas the variation around PAAS level in the Tveit schists is in contrast to the other areas. Apart from the quartz-rich gneisses and one schist from the Flekkefjord schists, there is a roughly linear increase in the Cr content with increasing TiO<sub>2</sub> and FeO<sub>T</sub>. One possible explanation is an additional amount of resistant residual minerals (chromite?) which are common in heavy sand deposits. The high Cr contents indicate a mafic source rock. In the silica-poor rocks, the high Cr and V contents may be explained by the tendency to adsorption in clay minerals, as heavy resistant minerals are not likely in a clay-dominated environment and increasing amounts of clay thus provide an opportunity for larger concentrations of these elements.

*Manganese* is known from residual clay deposits and deep-sea manganese nodules, but large deposits are rare. It differs from Fe by having an additional tetravalent ion giving rise to MnO<sub>2</sub> which is stable at high redox potentials, regardless of pH. Mn is dissolved during weathering and remains as Mn<sup>2+</sup> as long as the solution is only slightly acidic and not too oxidising. The negative Mn anomalies in the Flekkefjord and Tveit samples may indicate that the environment there was only slightly acidic and not too oxidising. Comparison between the Eh-pH diagrams for Mn and Fe may explain their separation during sedimentary processes (Krauskopf & Bird 1995) and will be outlined in connection with the discussion of the behaviour of iron.

*Iron* and its minerals have different stability fields from the Mn minerals in an Eh-pH diagram, which shows that hematite will precipitate in a large field of acidic and moderately oxidising conditions, while Mn<sup>2+</sup> remains in solution under the same conditions. The positive iron anomalies and high Fe/Mn ratios for most samples (which range between 85:1 and 147:1) may indicate that the prevailing conditions were moderately oxidising with stable or slowly changing pH. Exceptions are the Søgne schists with Fe/Mn ratios from 50:1 to 61:1 which is within the range of the total crust ratio of 50:1 and the upper continental crust ratio of 58:1 (Taylor & McLennan 1981, McLennan 1989). These ratios support a contribution from different source rocks. Within the same

level is one sample from Tveit (G25-6) (Fe/Mn ratio of 59:1) and the most quartz-rich gneiss which has a Fe/Mn ratio of 57:1. The Fe/Mn ratios of these rocks also suggests homogenisation, either due to recycling and/or mixing.

*Nickel* is mostly known from sulphide deposits in noritic and ultrabasic rocks. Another source of small amounts of nickel may be volcanic hydrothermal brines in an oceanic environment (Gross 1980). Only the Søgne schists have distinctly positive Ni ratios, whereas the Flekkefjord schists have only a slight positive tendency and all the Tveit schists have negative ratios. All the other gneisses have small Ni contents. Exponential increase of Ni with increasing  $TiO_2$ , supports the suggestion that the Søgne and possibly also the Flekkefjord schists are weathered products from an originally mafic or possibly even an ultramafic source rock. Some influence of hydrothermal brines cannot be totally dismissed. The Tveit schists may have been derived from a less mafic source or the Ni might have been diluted as a result of mixing with felsic source rocks.

### Interpretation of element geochemistry

Considering all the elements together in a sedimentary context allows a tentative picture to be drawn. The trace and transition element contents are within the range of clay sediments, so they do not contradict the interpretation that clay-rich sediments may be the precursors to the sillimanite schists. The gneisses probably had a considerable amount of quartz and also some feldspar in a clay matrix.

Some of the anomaly patterns may be explained by known sedimentary processes. The high ionic potential for phosphorus explains its deficiency if fluid conditions prevailed. The positive ratio in one of the quartz-rich gneisses may be explained by the presence of highly resistant phosphates such as monazite and/or xenotime. Positive anomalies of V, Cr, Ba, Rb and K are explained by their adsorption to clay minerals, whereas Sr was removed in suspension.

The most extreme anomalies are found in the *Søgne biotite-garnet-sillimanite schists*. The large positive anomalies for Y are considered significant and suggest that conditions were ideal for xenotime overgrowth on zircons. The Fe/Mn ratios suggest a certain homogenisation, due either to recycling or mixing or both. The high Ti, V, Cr, Mn, Fe, and Ni contents indicate that mafic or perhaps even a component from an ultramafic source rocks were dominant.

The *Tveit biotite-garnet-sillimanite schists* show a similar pattern for trace elements as the Søgne schists, although with smaller anomalies and with larger variations within the sample population. They have the lowest contents of transition elements among the schists and negative anomalies for Mn. Variation around the PAAS level may indicate deposition of clay sediments receiving material from different source rocks, although mainly dominated by mafic and intermediate rocks, ranging from basalts to latites. There may possibly even be a component from felsic source rocks.

The positive enrichment ratios for almost all trace elements, apart from P and Sr, in the *Flekkefjord biotite-garnet-*

*sillimanite schists* also suggest a mixed sediment from a broad spectre of continental source rocks, although mafic rocks seem to have dominated unless sorting has operated on a large scale.

The precursors to the *quartz-sillimanite gneisses* were probably sand-clay mixtures with high values for Zr, Th and Y (and Ce and La in the least quartz-rich sample) which supports zircon enrichment in the sand fraction. If the source rocks were the same as for the schists, a high degree of grain-size sorting must have taken place. Quartz incorporates insignificant amounts of trace elements and a gradual increase in the quartz content will consequently dilute the trace element concentration. The zircon content will counteract this effect as it commonly contains Ce, Nb, Th and REE. Zircons may either arrive as detrital grains or grow authigenically in sedimentary environments where xenotime is observed to crystallise on its surface, thus explaining the high Y contents (McNaughton et al. 1999, Fletcher et al. 2000). The precursors to the *felsic sillimanite gneisses* may have been immature feldspar-rich sediments.

The major element geochemistry rules out some other possible models of origin for the sillimanite schists. Immature sediments, such as glacial clay or loess, can be excluded because the high CIA index suggests rather highly weathered sediments derived in a warm, humid climate. The garnet-sillimanite schists and gneisses cannot be simple metamorphic derivatives of bauxite deposits, as bauxites normally contain almost twice as much alumina as the schists. Lateritic bauxites contain more than 40%  $Al_2O_3$ , which is well above the level for the sillimanite schists. The  $SiO_2$  content is also much lower in bauxites.

Pelagic red clays can also be excluded since they have different element distributions than the sillimanite rocks (McLennan et al. 1990, Li 1991, 2000). Oceanic basalts, even if strongly weathered, did probably not provide a source rock unless major changes had taken place. Normalization to MORB data from Bevins et al. (1984) reveals that K, Rb and Ba are from 14 to 284 times more abundant in the sillimanite rocks than in the MOR basalts. Furthermore, they have a large surplus of Th, Nb, Ce and La (up to 135 times the MORB value), while Zr and Y are 2 to 4 times more abundant. Even though some elements are strongly concentrated during sedimentary processes, these anomalies suggest that the source rock for the sillimanite rocks had a considerably higher level of these elements than MORB. However, if a considerable degree of mixing has taken place, some elements from such a source rock cannot be entirely excluded.

Several trace elements common in continental rocks have high concentrations in the Flekkefjord schists and together with the quartz-rich gneisses and the more immature gneisses it is tempting to suggest near-continental source rocks from an active mountain chain. The Tveit schists probably developed in more stable settings, whereas the precursors to the Søgne schists were possibly deposited on a deep shelf at some distance from a landmass.

Even if the geological history of the sillimanite-bearing schists and gneisses remains somewhat elusive, there seems

to be ample support for the notion that clay-rich sedimentary precursors developed during weathering in a warm, humid environment.

## Conclusions

The field association between the *biotite-garnet-sillimanite schists* and quartzites and marbles in the easternmost localities implies a sedimentary origin for these schists. Based on comparison of the major and trace element distributions with shales and pelites from various parts of the world and different time periods, we are led by degree to the conclusion that there is no major obstacle to the presumption that the precursors contained a considerable amount of clay minerals. It is significant that the major element distribution in the *biotite-garnet-sillimanite schists* is very similar to both ancient and even more recent clay sediments. According to the high CIA-index, the precursors to most of the studied sillimanite-bearing rocks have been thoroughly weathered, probably in a warm, humid climate. The Søgne schists were probably derived from more mafic source rocks than the Flekkefjord schists, which again might have been derived from more mafic source rocks than the Tveit schists. If large-scale grain-size sorting had been efficient, homogeneous mafic rocks mixed with more or less felsic debris should also be able to explain the differences. Some main element plots may indeed indicate both sorting and mixing but the distinct differences in several elements points towards source rock differences in the three different areas. Furthermore, there are some indications of regional environmental differences.

However, mixing had probably been in operation during formation of the *quartz-garnet-sillimanite gneisses*, as elements from both felsic and mafic rocks are important in these rocks. The high silica content is reflected in a high quartz content and suggests that the precursor was probably a coarse-grained heavy sand fraction mixed with a clay fraction.

The sedimentary precursors to the *felsic garnet-sillimanite gneisses* may have been more immature sediments with a mixture of quartz-sand and feldspars with a limited content of clay minerals.

The geochemical analyses suggest that known sedimentological processes may explain the origin of the sillimanite-bearing rocks and the most viable model involves weathering, mixing and sorting altering the source rocks to more or less clay-dominated sediments with an additional batch of quartz and feldspars, thus yielding evidence favouring the suggestion that they represent true metasediments.

## Acknowledgements

This investigation is a part of a project supported by the Geological Survey of Norway (NGU) and the authors appreciate the help received from many past and present staff members from the Survey. In particular, we would like to thank Richard Wilson for many stimulating discussions and for correcting the English text. We also thank Henrik

Friis for discussions on the sedimentological aspects. For technical assistance with the illustrations we thank Lissie Jans, and Ingrid Aaes and Jette Villesen for help with the analytical work. The referees, Mogens Marker and Raimo Lahtinen, are thanked for very constructive criticism. Furthermore, we thank the editor, David Roberts, for many helpful suggestions and for his last-minute corrections to the manuscript and many helpful suggestions. His editorial work with several of the first author's manuscripts during the last two decades is also greatly appreciated.

## References

- Berzelius, J.J. 1824: Undersökning af några Mineralier; 1. Phosphorsyrad Ytterjord. *Kungliga svenska Vetenskaps-Akademien Handlingar Stockholm 1824*, 334-358.
- Bevins, R.E., Kokelaar, B.P. & Dunkley, P.N. 1984: Petrology and geochemistry of lower to middle Ordovician igneous rocks in Wales: a volcanic arc to marginal basin transition. *Proceedings of the Geological Association 95*, 337-347.
- Brookins, D.G. 1983: Eh-pH diagrams for the rare earth elements at 250 C and One Bar Pressure. *Geochemical Journal 17*, No. 5, 223-229.
- Brookins, D.G. 1989: Aqueous geochemistry of rare earth elements. In: Lipin, B.R. & McKay, G.A. (eds.): Geochemistry and mineralogy of rare earth elements. *Mineralogical Society of America; Reviews in mineralogy 21*, 201-225.
- Bondam, J. 1967: Undersøgelser vedrørende de geokemiske forhold i kaolinforekomsten ved Rønne på Bornholm. *Bulletin of the Geological Society of Denmark 17*, Part 3, 297-356.
- Cameron, E.M. & Garrels, R.M. 1980: Geochemical compositions of some Precambrian shales from the Canadian Shield. *Chemical Geology 28*, 181-197.
- Chen, D.F., Dong, W.Q., Qi, L., Chen, G.Q. & Chen, X.P. 2003: Possible REE constraints on the depositional and diagenetic environment of Doushantuo Formation phosphorites containing the earliest metazoan fauna. *Chemical Geology 201*, 103-118.
- Condie, K.C. 1993: Chemical composition and evolution of the upper continental crust: Contrasting results from surface samples and shales. *Chemical Geology 104*, 1/4, 1-37.
- Englund, J.-O. 1973a: Geochemistry and mineralogy of pelitic rocks from the Hedmark Group and the Cambro-Ordovician sequence, Southern Norway. *Norges geologiske undersøkelse 286*, 1-60.
- Englund, J.-O. & Jørgensen, P. 1973b: A chemical classification system for argillaceous sediments and factors affecting their composition. *Geologiska Föreningens i Stockholm Förhandlingar, 95*, 87-97.
- Falkum, T. 1966a: The complex of metasediments and migmatites at Tveit, Kristiansand. Geological investigations in the Precambrian of southern Norway. No. 1. *Norsk Geologisk Tidsskrift 46*, 85-110.
- Falkum, T. 1966b: Structural and petrological investigations of the Precambrian metamorphic and igneous charnockite and migmatite complex in the Flekkefjord area, Southern Norway. *Norges geologiske undersøkelse 242*, 19-25.
- Falkum, T. 1998: The Sveconorwegian magmatic and tectonometamorphic evolution of the high-grade Proterozoic Flekkefjord complex, South Norway. *Norges geologiske undersøkelse Bulletin 434*, 5-33.
- Fletcher, I.R., Rasmussen, B. & McNaughton, N.J. 2000: SHRIMP U-Pb Geochronology of autigenic xenotime and its potential for dating sedimentary Basins. *Australian Journal of Earth Sciences 47*, 845-859.
- Govindaraju, K. 1994: Compilation of Working Values and Sample Description for 383 Geostandards. *Geostandard Newsletter, Special Issue, July 1994*, 1-158.
- Govindaraju, K. 1995: Working Values with Confidence Limits for Twenty-Six CRPG, ANRT and IWG-GIT Geostandards. *Geostandard Newsletter, Special Issue, July 1995*, 1-32.
- Gromet, L.P., Dymek, R.F., Haskin, L.A. & Korotev, R.L. 1984: The "North American Shale Composition": its compilation, major and trace ele-

- ment characteristics. *Geochimica et Cosmochimica Acta* 48, 2469-2482.
- Gross, G.A. 1980: A classification of iron formations based on depositional Environments. *Canadian Mineralogist*, 18, 215-222.
- Herz, N. 1962: Chemical composition of Precambrian pelitic rocks, Quadrilátero Ferrífero, Minas Gerais, Brazil. *United States Geological Survey, Professional Papers*, 450-C, 75-78.
- Korsch, R.J., Roser, B.P. & Kamprad, J.L. 1993: Geochemical, petrographic and grain-size variations within single turbidite beds. *Sedimentary Geology* 83, 15-35.
- Krauskopf, K.B. & Bird, D.K. 1995: *Introduction to Geochemistry*. 3rd ed. McGraw Hill Inc., 647 pp.
- Li, Y.-H. 1991: Distribution patterns of the elements in the ocean: A Synthesis. *Geochimica et Cosmochimica Acta* 55, 3223-3240.
- Li, Y.-H. 2000: *A compendium of Geochemistry*. Princeton University Press, 475 pp.
- McArthur, J.M. & Walsh, J.N. 1984: Rare-earth geochemistry of phosphorites. *Chemical Geology* 47, 191-220.
- McLennan, S.M. 1989: Rare earth elements in sedimentary rocks: influence of Provenance and sedimentary processes. In: Lipin, B.R. & McKay, G.A.(eds.): *Geochemistry and mineralogy of rare earth elements*. *Mineralogical Society of America. Reviews in Mineralogy* 21, 169-200.
- McLennan, S.M., Taylor, S.R., McCulloch, M.T. & Maynard, J.B. 1990: Geochemical and Nd-Sr isotopic composition of deep sea turbidites: Crustal evolution and plate tectonic associations. *Geochimica et Cosmochimica Acta* 54, 2015-2050.
- McNaughton, N.J., Rasmussen B. & Fletcher, I.R. 1999: SHRIMP Uranium-Lead Dating og diagenetic xenotime in siliciclastic rocks. *Science* 285, 5424, 78-80.
- Nesbitt, H.W. & Young, G.M. 1982: Early Proterozoic climates and plate motions inferred from major element chemistry of lutites. *Nature* 299, 715-717.
- Nesbitt, H.W. & Young, G.M. 1989: Formation and diagenesis of weathering profiles. *Journal of Geology* 97, 129-147.
- Pettijohn, F.J. 1975: *Sedimentary Rocks*. 3rd ed. Harper & Row, New York, 628 pp.
- Ronov, A.B. & Migdisov, A.A. 1971: Geochemical history of the crystalline basement and the sedimentary cover of the Russian and American platforms. *Sedimentology* 16, 3/4, 137-185.
- Simonen, A. 1953: Stratigraphy and sedimentation of the Svecofennidic, Early Archean supracrustal rocks in Southwestern Finland. *Bulletin de la commission géologique de Finland* 160, 64 pp.
- Taylor, S.R. & McLennan, S.M.: 1981: The composition and evolution of the continental crust: rare earth element evidence from sedimentary rocks. *Philosophical Transactions of the Royal Society A301*, 381-399.
- Taylor, S.R. & McLennan, S.M. 1985: *The continental crust: its composition and evolution*. Blackwell, Oxford. 312 pp.
- Wright, J., Schrader, H. & Holser, W.T. 1987: Paleoredox variations in ancient oceans recorded by rare earth elements in fossil apatite. *Geochimica et Cosmochimica Acta* 51 637-644.